iScience

CellPress
OPEN ACCESS

Article

Occurrence of PFASs and its effect on soil bacteria at a fire-training area using PFOS-restricted aqueous film-forming foams

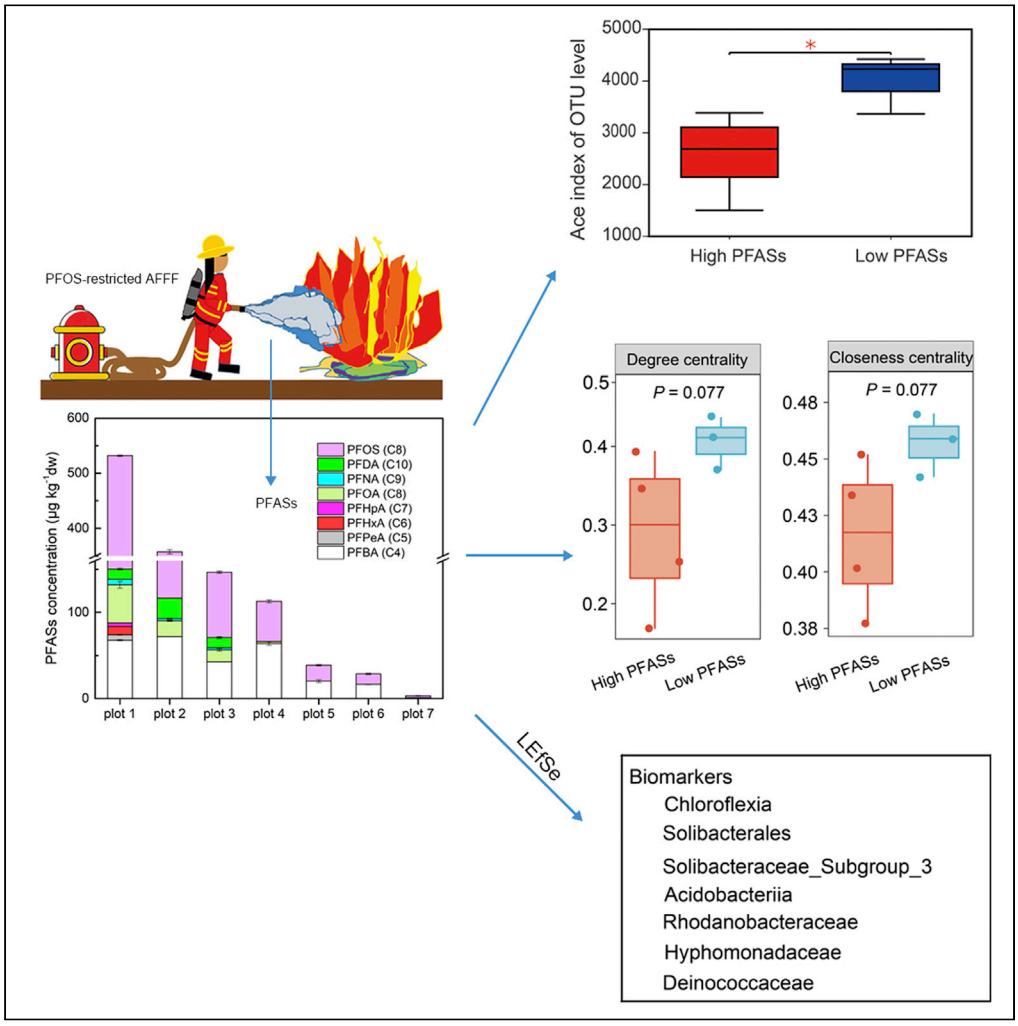

Lifeng Cao, Wenxin Xu, Ziren Wan, Guanghe Li, Fang Zhang

fangzhang@tsinghua.edu.cn

Highlights

PFOS was still the dominant PFAS despite the restriction by Stockholm Convention

PFASs played an important role in shaping bacterial community

High level of PFASs reduced the biodiversity and connectivity of soil bacteria

The extreme condition-tolerant bacteria were identified as biomarkers at the FTA

Cao et al., iScience 25, 104084
April 15, 2022
https://doi.org/10.1016/j.isci.2022.104084

iScience

CellPress
OPEN ACCESS

Article

Occurrence of PFASs and its effect on soil bacteria at a fire-training area using PFOS-restricted aqueous film-forming foams

Lifeng Cao,[1] Wenxin Xu,[1] Ziren Wan,[1] Guanghe Li,[1] and Fang Zhang[1,2,*]

SUMMARY

Fire-training areas (FTAs) are an important source of perfluoroalkyl and polyfluoroalkyl substances (PFASs) pollution. However, the effect of PFASs on soil bacterial communities remains limited. Here, we detected the PFASs in soils ranging from 3.4 to 531.7 μg kg^{-1} dry weight in seven plots at an FTA where PFOS-restricted aqueous film-forming foams (AFFFs) have been used for 6 years. PFOS was still the dominant homologue despite the restriction by Stockholm Convention, but it was almost three orders of magnitude lower than that in previous studies. PFASs played an important role in shaping the bacterial community, and high levels of PFASs (>100 μg kg^{-1} dw) reduced the biodiversity and connectivity of soil bacteria. The extreme condition-tolerant bacteria were identified as biomarkers at the FTA. Our study provides valuable insights into the effect of PFOS-restricted AFFFs on soil bacterial communities at the FTA.

INTRODUCTION

Perfluoroalkyl and polyfluoroalkyl substances (PFASs) are a group of manmade organic chemicals containing fully or partially fluorinated carbon chains with a variety of neutral or ionic functional groups (Wang et al., 2017). PFASs can the reduce surface tension and facilitate foam spreading and fire smothering (Wang et al., 2013), thus they have been added into aqueous film-forming foams (AFFFs) since the1960s to extinguish liquid fuel fires at fire-training areas (FTAs). As large volumes of PFASs enter into the environment during the repeated use of AFFF, PFAS have been frequently detected in soil and groundwater at the FTAs (Brusseau et al., 2020; García et al., 2019), The maximum reported concentrations for perfluorooctane sulfonic acid (PFOS) ranged up to several hundred mg kg^{-1}, which were generally orders-of-magnitude higher than those at other contaminated sites (Brusseau et al., 2020). The most frequently detected PFASs were PFOS and perfluorooctanoic acid (PFOA), which have been proven to be bioaccumulative and toxic in higher animals including humans (Ahrens et al., 2019). In 2009, PFOS was listed in Annex B of the Stockholm Convention, and a complete ban on the use of AFFFs containing PFOS was suggested and enforced by several major manufacturers in 2011 (UNEP, 2009). However, in the FTAs which used PFOS-restricted AFFFs after 2011, information remains limited regarding occurrence of PFASs and its effect on soil bacteria.

PFASs are generally resistant to microbial degradation and persist in soil (Huang and Jaffé, 2019). The effects of PFASs on soil microorganisms have drawn extensive attention because the activity, biodiversity, and composition of microorganisms play critical roles in maintaining many biogeochemical processes or indicating the soil properties. Researches have indicated that the long-term exposure to PFASs resulted in a significant decrease in the biodiversity of soil microbial community, leading to the enrichment of more PFASs-tolerant bacteria, such as Proteobacteria, Acidobacteria, and Bacteroidetes (Bao et al., 2018; Qiao et al., 2018). The soil community diversity decreased in plant-soil-water systems when three concentrations of eight PFASs mixtures (7.46 μg L–1, 5,165 μg L–1, and 51,650 μg L–1) were added into soil, with a clear distinction in bacterial community structure between the soils with and without PFAS addition (Zhang et al., 2019b). A field survey revealed that PFOA contaminated sediment at 456.20 μg kg–1 dry weight (dw) also decreased community diversity (Sun et al., 2016). However, the effects of PFASs on community biodiversity might be dependent on the concentration. With 90 days of exposure, the biodiversity of soil microbial communities increased with the 250 μg L–1 PFOS treatments (Xu et al., 2021b).

[1]State Key Joint Laboratory of Environmental Simulation and Pollution Control, State Environment Protection Key Laboratory of Microorganism Application and Risk Control, School of Environment, Tsinghua University, Beijing 100084, China

[2]Lead contact

*Correspondence: fangzhang@tsinghua.edu.cn

https://doi.org/10.1016/j.isci.2022.104084

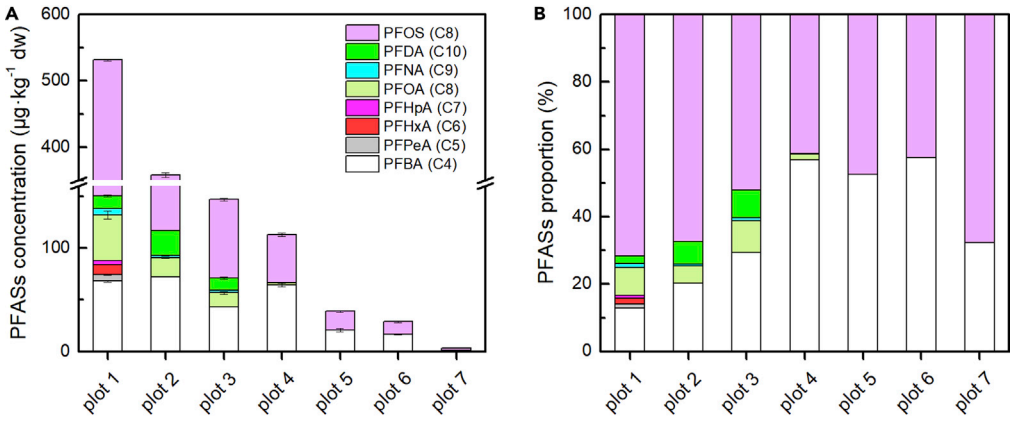

Figure 1. PFASs concentration (A) and proportion (B) at seven plots for PFDA, PFNA, PFOA, PFHpA, PFHxA, PFPeA, PFBA, and PFOS. PFASs concentration presents an average value of three samples at each plot.

PFASs generally showed a negative effect on bacterial functions. In a methanogenic and mixed culture, reductive dechlorination of trichloroethene (TCE) for *Dehalococcoides* was significantly inhibited when exposed to concentrations representative of PFASs source zones (total of >66 mg L–1 for 11 PFASs analytes, 6 mg L–1 each) (Weathers et al., 2016). When an anaerobic digester community were exposed to PFASs (50 mg L–1) and a co-contaminant (2,4-dichlorophenol, DCP), PFASs could alter the toxicity of DCP, inhibit DCP degradation, decrease the number of methanogens, and change the microbial community structure (Fitzgerald et al., 2019). A greenhouse experiment confirmed that PFOS (10 mg kg^{-1} soil) inhibited soil enzyme activity and further destroyed the cellular structure, immune system, and gene expression of soil bacteria (Qiao et al., 2018). To date, these studies have primarily focused on the effect of PFASs on bacteria in labs and the occurrence of PFASs in soil and groundwater at the FTAs. The knowledge about the effect of PFASs on soil bacteria remains limited at the FTAs, including biodiversity, composition, and functions.

To address the limited information of the effect of PFASs on soil bacteria and the concentrations of PFASs in soils at the FTA which used PFOS-restricted AFFFs after 2011, a fire-training base in Shanghai, China was selected as the study area. This base was established in December 2012 and has been used for firefighting training activities since 2013. We detected the concentrations of PFASs in top surface soils and sediments, assessed potential impacts of PFASs on soil community diversity, composition, and functions by high-throughput sequencing, and revealed the relationship between bacterial community and soil physical and chemical properties.

RESULTS

Characteristic of PFASs concentrations at each plot

An FTA in Shanghai, China was selected as the study area with seven sampling plots, where plots one to four were located at firefighting zones and other three plots were far away from the firefighting zones (Figure S2). Plots one and two were the area of simulated oil tank fires where hydrocarbon-based fuel fires were extinguished by using AFFFs. Eleven PFASs analytes were determined (Tables S3 and S4), and the total PFASs concentrations (∑PFASs) ranged from 3.4 μg kg^{-1} dw to 531.7 μg kg^{-1} dw (Figure 1A). The concentrations of ∑PFASs in this study at the FTA were much lower than those reported in previous studies. ∑PFAS in each sample from plots one to four was more than 112.9 μg kg^{-1} dw and much higher than that from plots 5–7. Soils from the park (plot 7) had the lowest ∑PFASs which was only 3.4 μg kg^{-1} dw. It suggests that repeated use of AFFFs at the firefighting zones led to high PFASs pollution in surrounding soils.

PFOS was the dominant homologue and counted for more than 41.2% of the ∑PFASs in all samples. The maximum concentration of PFOS occurred at plot one which was 381.3 μg kg^{-1} dw. PFOS accounted for 41.2–71.7% of the ∑PFAS in all samples (Figure 1B). PFBA was also frequently detected, accounting for 12.8–57.6% of the ∑PFAS at all samples. The highest concentration of perfluorobutanoic acid (PFBA) was 72.1 μg kg^{-1} at the plot 2. For PFOA, plot one also presented the highest PFOA concentration at

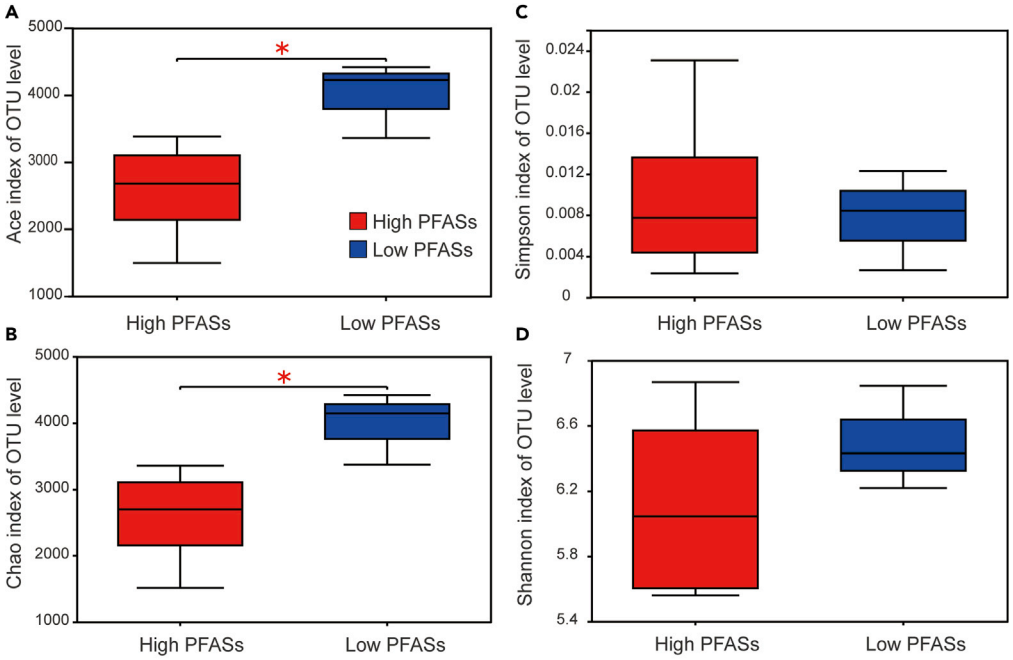

Figure 2. The biodiversity indexes for Ace index (A), Chao index (B), Simpson index (C) and Shannon index (D) between low PFASs group and high PFASs group. High PFASs group including plot 1–4: more than 100 μg kg^{-1} PFAS was detected in the dry weight soils; Low PFASs group including plot 5–7: less than 100 μg kg^{-1} PFASs was detected in the dry weight soils. Significant differences are indicated by *p < 0.05.

44.2 μg kg^{-1} dw. In addition, several long-chain perfluoroalkyl acids (PFAAs) such as perfluorononanoic acid (PFNA, C9) and perfluorodecanoic acid (PFDA, C10) were detected in the plots 1–3. Notably, seven PFAAs (C4-C10) were all observed at the plot 1. The detailed concentrations of each PFAS are presented in Table S2.

Negative association between alpha diversity and high level of PFASs

A total of 459,881 quality-filtered and chimera-checked 16S rRNA gene sequences were obtained with an average length of 417 bp across all samples. The number of 16S rRNA sequences obtained per sample varied from 55,093 to 73,007. A total of 16,304 bacterial OTUs were identified across this study (Figure S3).

Samples were divided into high PFASs group (>100 μg kg^{-1}, plot 1–4) and the low PFASs group (<100 μg kg^{-1}, plot 5–7). Bacterial community richness (Chao1 and ACE) and diversity (Shannon and Simpson) index values were compared between the high PFASs group and the low PFASs group. The indexes of alpha diversity at each plot are shown in Figure S4. The mean ACE index was 4,000 ± 563 in the low PFASs group, which was higher than that of 2,558 ± 826 in the high PFASs group (Figure 2A). The mean Chao1 index was 3,979 ± 542 in the low PFASs group and was 2,565 ± 813 in the high PFASs group (Figure 2B). The Chao1 and ACE index indicated that bacterial community richness in the low PFASs group was significantly higher than those in the high PFASs group ($p < 0.05$).

Similarly, the community biodiversity in the low PFASs group was higher than that in the high PFASs group. The mean Simpson index was 0.008 ± 0.005 in the low PFASs group and was 0.01 ± 0.009 in the high PFASs (Figure 2C). The mean Shannon index was 6.50 ± 0.32 in the low PFASs group, which was also higher than that in the high PFASs group (6.12 ± 0.65) (Figure 2D). These results suggest that high concentrations of PFASs (∑PFASs >100 μg kg^{-1} dw) in soil significantly decreased bacterial community biodiversity.

Composition of the soil bacterial community at the FTA

The composition of the bacterial community showed an obvious difference between samples. Percentage of community abundance at each sample at phylum level and at family level was shown in Figure S5. At

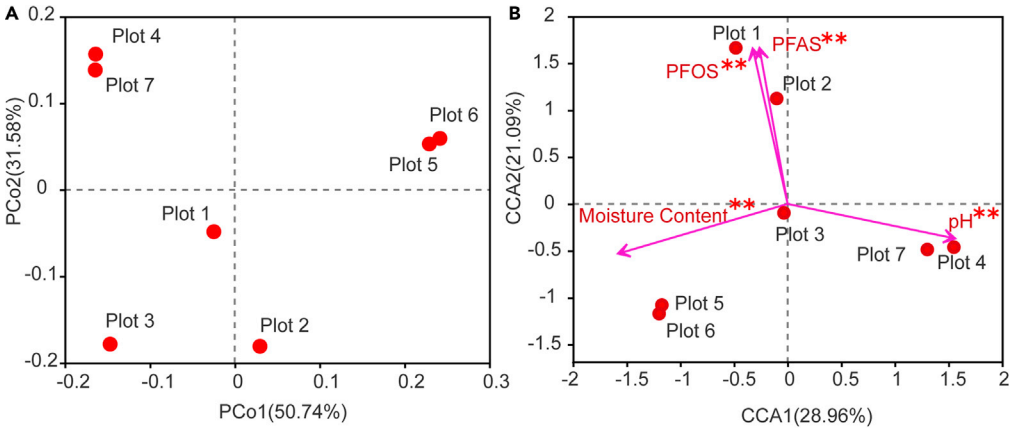

Figure 3. Principal coordinates analysis (PCoA)

(A) at class level and canonical correspondence analysis (CCA).

(B) based on relative abundance of OTUs in each plot. CCA analysis differentiates the contributing physicochemical factors (pH, MC, PFOS, and ∑PFAS) to the shifts in microbial community at the FTA. The values of axes one and two are the percentages explained by the corresponding axis. Significant differences are indicated by **$p < 0.01$.

phylum level, Proteobacteria was the dominant phylum at all plots, accounting for 29.4–47.7% of the phyla (Figure S5A). The other top five phyla included Chloroflexi (11.1–22.9%), Actinobacteria (7.5–17.5%), Acidobacteria (5.4–23.6%), Bacteroidetes (2.4–8.4%), and Cyanobacteria (0.4–7.5%). At family level, the most abundant family was Steroidobacteraceae, accounting for 1.0–16.4% of total sequences (Figure S5B). Accordingly, *Steroidobacter*, belonging to the Steroidobacteraceae family, was the most abundant genus at the plot 2 (15.6%) and at the plot 3 (4.8%) (Figure S5). A large proportion of OTUs could not be assigned to specific genus at top 19 genera based on the current Silva database (Figure S6).

The beta diversity at class level was analyzed by Principal coordinates analysis (PCoA). The first two axes (PCo1 and PCo2) explained 82.3% of the total variance in the bacterial species at the seven plots (Figure 3A). PCo1 explained 51.7% of the variation, whereas PCo2 explained 31.5%. Based on PCoA results, the seven plots were classified into three groups, mainly attributed to the varied sources of samples. The plots one to three were located at the fire-training zones. The soils from plot four and seven were surrounded by vegetation, whereas plots five and six were sediment of the river (Figure 3).

Enhanced metabolism in the high level of PFASs contaminated soils

To evaluate the effect of PFASs on bacterial functions, the abundance of metabolism involved in carbon metabolism, nitrogen metabolism, benzoate degradation, and chlorinated solvents degradation were compared between the high and low PFASs sample groups. The abundance of metabolism at each plot is shown in Figure S7. Carbon and nitrogen metabolism in the high PFASs group were significantly higher than those in the low PFASs group ($p = 0.034$). The abundance of carbon metabolism was 3,428,561 ± 193,378 in the high PFASs group, which was 26.1% higher than that in the low PFASs group (Figure 4A). The abundance of nitrogen metabolism was 390,878 ± 289,64 in the high PFASs group, 26.4% higher than that in the low PFASs group (Figure 4B).

Because co-contaminants including chlorinated solvents and phenyl fuels have been detected at AFFF-contaminated sites (Guelfo and Higgins, 2013), the abundance of xenobiotic biodegradation and metabolism for benzoate and chlorinated solvents was also compared between the high PFASs group and the low PFASs group. However, all of these contaminants were below the detection limits (data not shown). The main reason was likely that chloroalkane, chloroalkene, and benzoate in the top surface soil were easily degraded by microbes or volatilized into air (Bugna et al., 2005; Kao and Prosser, 1999). The abundance of benzoate degradation in the high PFASs group was 46.8% higher than that in the low PFASs group (Figure 4C), whereas the abundance of chloroalkane and chloroalkene degradation in the high PFASs group was 53.9% higher than that in the low PFASs group (Figure 4D). These results indicate that fire training exercises significantly enhanced metabolism involved in carbon metabolism, nitrogen metabolism, benzoate degradation, and chloroalkane and chloroalkene degradation ($p = 0.034$).

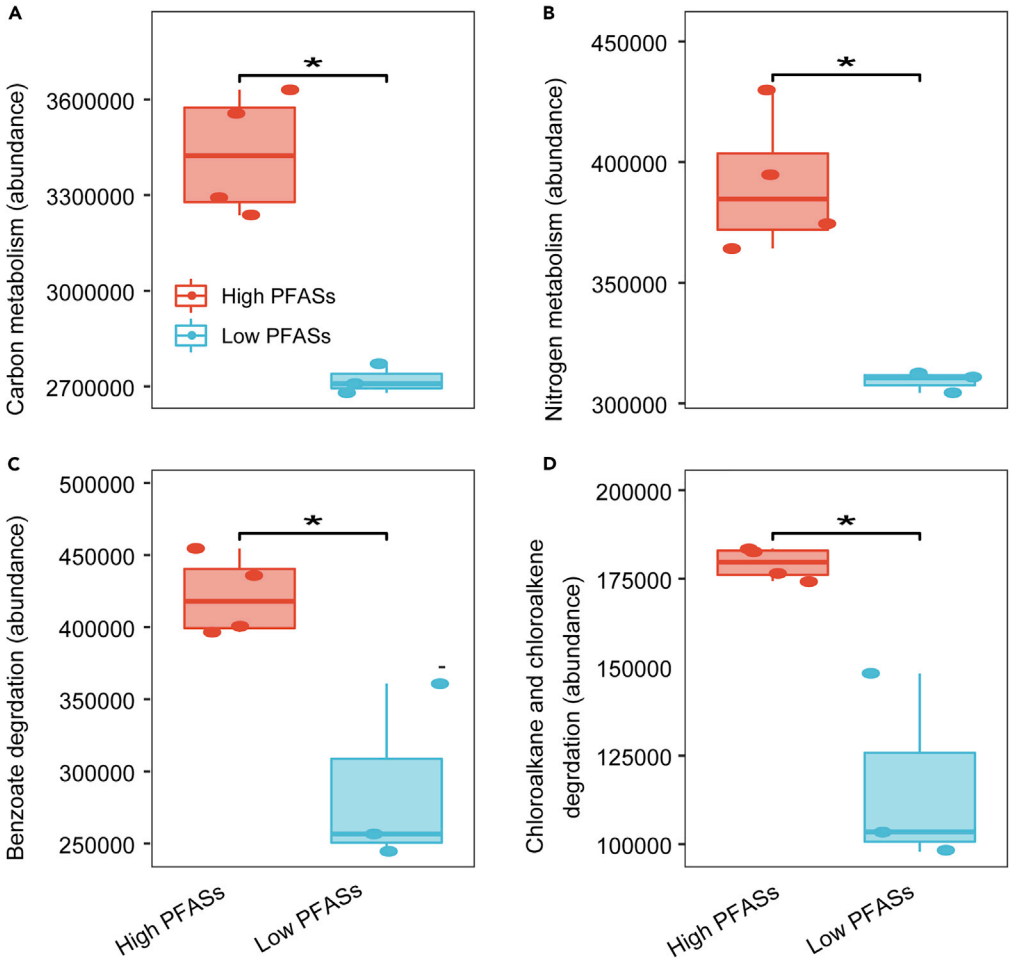

Figure 4. The abundance of metabolism involved in carbon metabolism (A), nitrogen metabolism (B), benzoate degradation (C), and chloroalkane and chloroalkene degradation (D) between the low PFASs group and the high PFASs group. Significant differences are indicated by *p < 0.05.

Relationships between bacterial community and environmental characteristics

Relationships between microbial community structure and environmental characteristics were investigated by canonical correspondence analysis (CCA). Physicochemical properties of soil at each sampling plot were analyzed and listed as Table S1. CCA revealed that the microbial community structure was formed by selected environmental characteristics. As shown in Figure 3B, moisture content ($p = 0.006$), pH ($p = 0.009$), PFOS ($p = 0.008$), and PFASs ($p = 0.009$) significantly affected the bacterial community structure. PFOS and ∑PFAS had the greatest influence on the soil microbiota of plot 1 and 2, which was consistent with the result that highest concentrations of PFAS were detected at the plot one and 2. As plot five and six were from sediment which had the highest moisture content (Table S1), CCA showed that moisture content had the greatest effect on the microbiota of plot five and 6. At the plot four and seven where soils with a higher alkalinity (pH>8.14), pH had the greatest influence on soil microbiota. However, the four environmental factors had a weak effect on soil microbiota of plot 3.

Spearman correlation analysis indicated that most environmental factors in soils were significantly correlated with the proportions of the top 15 phyla (Figure 5). Except IC and PFBA, all the other environmental factors showed significant correlation with one or more phyla; however, Actinobacteria, Bacteroidetes, Firmicutes, and Nitrospirae demonstrated an insignificant correlation with all environmental characteristics. Only Chloroflexi showed a significant positive correlation with PFOS and PFASs. Although PFBA presented a relatively high concentration at each plot, it showed no significant correlation with all the top 15 phyla.

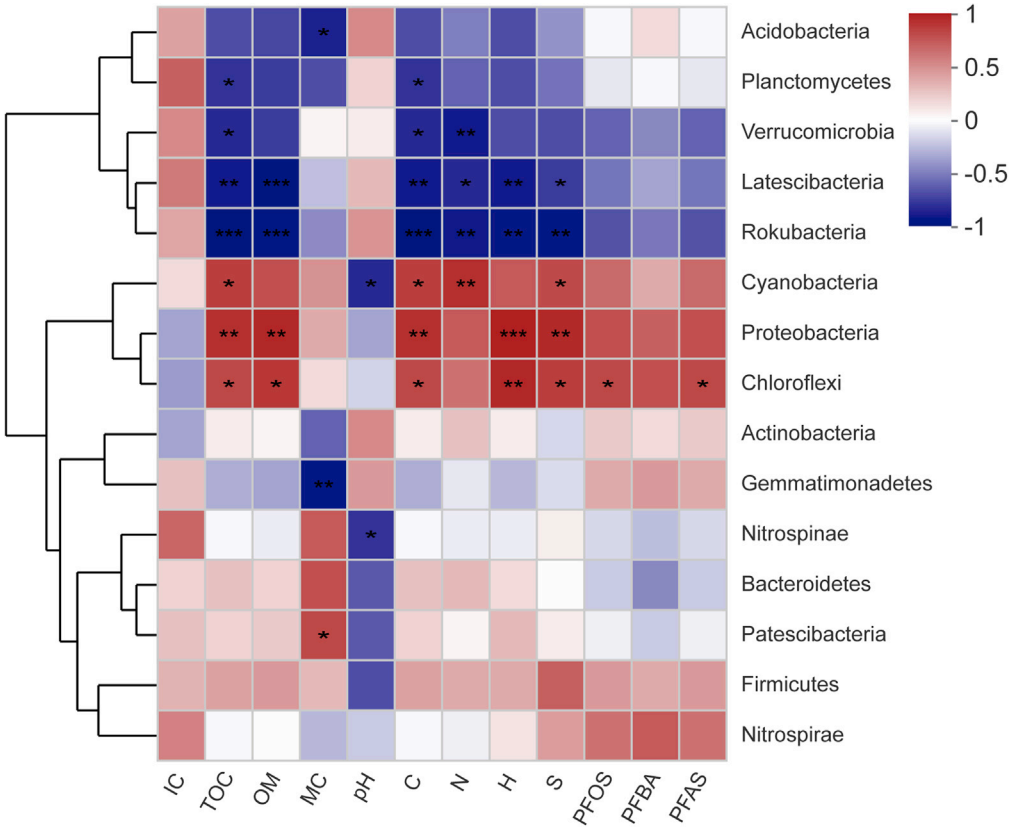

Figure 5. Spearman correlation heatmap of the top 15 phyla and soil properties and concentrations of PFASs.
Inorganic carbon (IC), total organic carbon (TOC), organic matter (OM), total carbon (C), total nitrogen (N), total hydrogen (H), total sulfur (S), and moisture content (MC). The X and Y axis are environmental factors and phyla. R in different colors to show, the right side of the legend is the color range of different R values. Significant values are shown as: *p < 0.05; **p < 0.01; ***p < 0.001.

Microbial communities with statistically significant differences

To identify the specialized communities in the two groups, the LEfSe tool was used to analyze microbial community data from the phylum to the family level (Figure 6). LEfSe analysis confirmed the significant enrichment of Rhodanobacteraceae, Hyphomonadaceae, D05-2, Acidobacteriia, Solibacterales, Solibacteraceae_Subgroup_3, SBR1031, Chloroflexia, and Deinococcaceae in the high PFASs group ($p<0.05$). On the other hand, Bacillales, Bacteroidetes, Bacteroidia, Sphingobacteriales, Desulfuromonadales, RCP2-54, norank family from RCP2-54 order, Spongiibacteraceae, Oceanospirillales, Halomonadaceae, norank family from Gaiellales, Verrucomicrobiales, Rubritaleaceae, Methylomirabilales, and Methylomirabilaceae were significantly enriched in the low PFASs group ($p<0.05$).

The topological impacts of PFASs accumulations on soil bacteria

As the topology of the co-occurrence network could reflect interactions between microorganisms, the co-occurrence network was constructed (Figure S8) and the topological parameters such as degree centrality, closeness centrality, and betweenness centrality were calculated (Figure 7). The degree centrality for a node is simply its degree, which presents the number of adjacent edges in each sample node (Greenblum et al., 2012). The average degree of the sample node was 3,076 $\pm$ 258 in the low PFASs group, higher than that of 2,203 $\pm$ 759 in the high PFASs group (Figure S9). The normalized degree centrality in the low PFAS group (0.41 $\pm$ 0.04) was 39.6% higher than that in the high PFASs group (0.29 $\pm$ 0.1). The closeness centrality is the inverse of the average shortest distance between the node and all other nodes, which was 0.46 $\pm$ 0.01 in the low PFASs group and 0.42 $\pm$ 0.03 in the high PFAS group. The betweenness centrality that represents the degree to which nodes stand between each other

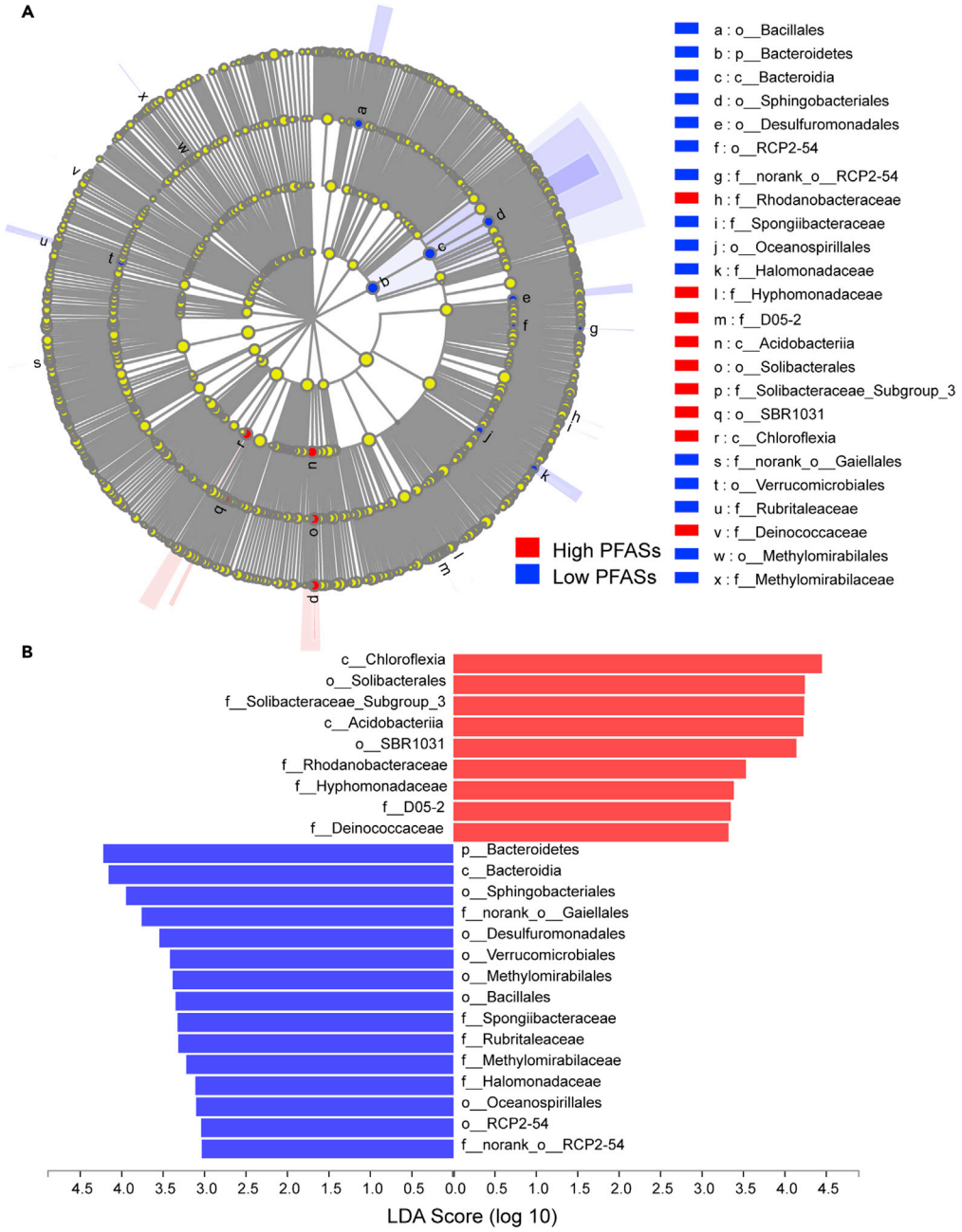

Figure 6. Identification of the biomarkers from high PFASs group and low PFASs group using the LEfSe analysis. Cladogram showing the phylogenetic distribution of the bacterial lineages associated with different concentrations of PFASs in soils

(A) Linear discriminant analysis (LDA) coupled with effect size measurements (LEfSe) analysis identified biomarkers with a p-value < 0.05 and LDA scores ≥3 in bacterial communities associated with PFASs concentrations in soils.

(B) Circles indicate phylogenetic levels from phylum to family.

followed a similar trend that the low PFASs group had a higher betweenness centrality than that of the high PFAS group (0.25 ± 0.03 vs 0.18 ± 0.09). High values of these topological parameters indicate a core location (intensive connections) of this node in the network, whereas low values indicate a more peripheral location. These results collectively suggested that high levels of PFASs in soils decreased the intensive connection of soil bacteria in the PFAS contaminated soil.

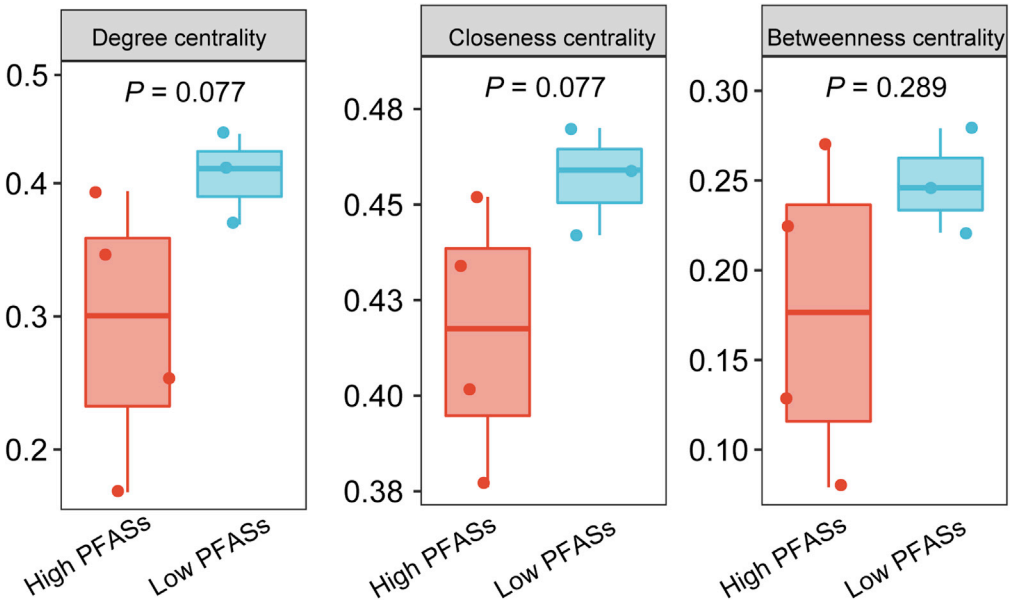

Figure 7. The topological parameters between low PFASs group and high PFASs group

DISCUSSION

The stockholm convention for PFOS pollution mitigation

To compare concentrations of PFASs with reported concentrations, an overview of the literature data for maximum PFOA and PFOS at the FTAs was presented in Table 1. Data were reported for a total of 15 FTAs across the six countries. PFOA and PFOS were the most prevalent PFASs species at the FTAs reported for all the studies. The maximum reported concentrations for PFOA ranged from 2 to 50,000 μg kg^{-1} dw, whereas they ranged from 381 to 373,000 μg kg^{-1} dw for PFOS. The maximum concentrations of PFOS exceeded 373 mg kg^{-1} dw in the United States, although the period was unclear for this contaminated site. In an FTA with a period of 27 years from Australia, the concentration of PFOS was more than 200 mg kg^{-1} dw. The high PFOA concentrations that exceeded 10 mg kg^{-1} dw in the FTA were only observed in the United States. The concentrations of PFOS in the FTAs from Norway and Sweden were less than 9 mg kg^{-1} dw.

In this study, PFOS was the most dominant PFASs present in all soil samples at the FTA (Figure 1), which was consistent with previous results (Sharifan et al., 2021). The maximum concentration of PFOS was only 381 μg kg^{-1} dw, which was much lower than that in other countries. The maximum concentration of PFOS at the FTA was several magnitudes lower than that at the FTAs in the United States (Brusseau et al., 2020), likely because of the shorter pollution duration. According to the period of pollution provided in Table 1, the FTA in this study had the shortest pollution duration (6 years).

Since the Stockholm convention, a complete ban on the use of AFFF containing PFOS has been suggested and enforced by several major manufacturers in 2011 (UNEP, 2009); therefore, application of AFFFs was gradually replaced by PFOS-restricted AFFFs after 2006 in China (Zhang et al., 2012). PFOS was the primary PFASs in the original 3M formulations, ranging from 4.9 to 11.4 g L^{-1} (Houtz et al., 2013). The selected fire-training base in this study was established in December 2012 and has been used for firefighting training activities since 2013. PFOS in the raw AFFFs purchased from a Chinese firefighting equipment company was detected ranging from 118 to 434 mg L^{-1}, which are almost two orders of magnitude lower than that in the original 3M formulations (Figure S1). This result indicates that the application of PFOS-restricted AFFFs appreciably reduced PFOS concentrations at the FTAs.

High levels of PFASs pollution results in biodiversity and interaction loss

A negative association between high concentration of PFASs (∑PFASs > 100 μg kg^{-1} dw soil) and bacterial community diversity was observed at the FTA (Figure 2). Some sensitive microbial species might be phased

Table 1. Overview of previously reported PFASs soil contaminations (potentially incomplete) at the fire-training area (FTA) including information about country, pollution time (where available), major detected PFASs species and their maximum concentrations

Period (years)	Max. PFOA Conc. (μg kg^{-1})	Max. PFOS Conc. (μg kg^{-1})	Time	Country	Reference
12	13	2,600	1989–2001	Norway	(Hale et al., 2017)
19	141	8,924	1988–2006	Norway	(Aasen et al., 2008)
–	12	1,905	n.p	Norway	(Kärrman et al., 2011)
26	n.p	6,500	1990–2016	Norway	(Høisæter et al., 2019)
21	2	486	1985–2005	Sweden	(Bergström, 2014)
48	287	8,520	1946–1994	Sweden	(Filipovic et al., 2015)
48	11,484	36,534	1942–1990	USA	(McGuire et al., 2014)
20	140	9,700	1970–1990	USA	(Anderson et al., 2016)
–	50,000	373,000	n.p	USA	(Brusseau et al., 2020)
22	40	4,000	1988–2010	Australia	(Baduel et al., 2017)
–	55	13,400	n.p	Australia	(Bräunig et al., 2019)
27	1,259	223,982	1983–2010	Australia	(Baduel et al., 2015)
–	90	10,000	n.p	Australia	(Casson and Chiang, 2018)
28	514	55,197	1987–2015	France	(Dauchy et al., 2019)
6	44	381	2013–2019	China	This study

n.p.= information not provided.

out with a long-term exposure to PFASs, which might account for the decrease of bacterial community biodiversity. Our result is consistent with previous studies that PFASs at high concentrations significantly decreased the bacterial community diversity. In previous studies which investigated the effect of PFOA or PFOS on bacteria, the Shannon index in samples with 5 mg L^{-1} PFOA (2.83 $\pm$ 0.06) was significantly lower than that in samples without PFOA (3.86 $\pm$ 0.08), whereas the Shannon and Chao one index in soils with 10 mg kg^{-1} PFOS were lower than those in soils with PFOS ranging from 10 to 1000 μg kg^{-1} (Qiao et al., 2018; Zhang et al., 2019b). In addition, a higher content of PFOS in soils had significant negative correlations with bacterial community richness and diversity in the chrome-plating factory (Bao et al., 2018). Although a specific concentration of PFASs decreased biodiversity wasn't given by the studies, higher concentrations of PFASs would usually reduce biodiversity in the same area.

The topological parameters demonstrated that high levels of PFASs pollution apparently simplified soil bacterial interactions (Figure 7). A recent study revealed that the PFOS-treated soil increased the intensive connection of the network than that in the PFOA treated soil (Xu et al., 2021b). However, the topological features in soil microbial co-occurrence network at the fire training area remained largely unknown. Lower betweenness centrality values were observed in the high PFASs group than those in the low PFASs group. OTUs with low betweenness centrality values represent microorganisms that are located away from the core of the network, compared to other OTUs (Greenblum et al., 2012). The closeness centrality is also used to identify important positions within the co-occurrence network (Chea and Livesay, 2007). Lower closeness centrality values were observed in the high PFASs group than those in the low PFASs group. These suggest that the soil microbes from the low level of PFASs contaminated soil were more often located in core, central positions within the network than those from the high PFASs contaminated soil. Although the topological features of the occurrence network indicated that high concentration PFASs in soils decreased the potential species interactions, revealing the true interaction processes and underlying mechanisms will require additional evidence by more targeted manipulative experiments.

Stronger metabolism in high levels of PFASs contaminated soils

The bacterial functions involved in carbon metabolism, nitrogen metabolism, and xenobiotic biodegradation and metabolism in the high PFASs group were significantly higher than those in the low PFASs group in this study, which was inconsistent with previous studies. Previous works showed that PFASs had a toxic effect on bacterial functions by means of membrane disruption, DNA damage, and oxidative damage

(Liu et al., 2016). A high level of PFOS (ppm level) not only inhibited soil enzyme activity but also destroyed the cellular structure, immune system, and gene expression of soil bacteria (Qiao et al., 2018). Reductive dechlorination by *Dehalococcoides* was significantly inhibited when exposed to concentrations of PFASs at > 66 mg L^{-1} (Weathers et al., 2016). The PFASs concentration at 50 mg L^{-1} could not only inhibit the activity of methanogens, but also inhibit the biodegradation of dichlorophenol (Fitzgerald et al., 2019). Exposure of 10 mg kg^{-1} PFOS reduced soil sucrase by 30% and damaged the soil ammonia oxidation process (Qiao et al., 2018). The toxicological analysis revealed that PFOS was responsible for AFFF toxicity (Fitzgerald et al., 2019).

In this study, PFOS was the dominant PFASs species in all samples, but the toxic concentrations (ppm level) reported by previous studies exceed our maximum value (381 μg kg^{-1} dw PFOS) by orders of magnitude. It indicates that the level of PFOS had no obvious inhibition to bacterial functions in this study. Compared with PFASs, the co-contaminants such as TCE, benzene, toluene, ethylbenzene, and xylenes are easy to microbial degradation (Bugna et al., 2005; Kao and Prosser, 1999). Therefore, the abundances of xenobiotic biodegradation and metabolism in the fire training zone were significantly higher than those in the area near the fire training zone.

PFOS plays an important role on shaping bacterial community structure

High levels of PFOS only at the plot 1 (381 μg kg^{-1} dw) and 2 (241 μg kg^{-1} dw) significantly affected the soil bacterial community structure (Figure 3B). The effect of PFASs on bacterial community structure in soils, sediments, and water were reported by many research works at field scale and laboratory scale. They showed that high levels of PFASs (≥ μg L^{-1} or kg^{-1} level) obviously changed bacterial community structure in soils, sediments, and water (Qiao et al., 2018; Weathers et al., 2016; Zhang et al., 2019a, 2019b). The maximum concentration of PFOS in soils reached 381 μg kg^{-1} dw in this study, thus PFOS definitely played an important role in shaping bacterial community structure. However, low levels of PFASs (below μg L^{-1} or kg^{-1} level) had no or slight effects on shaping bacterial community structure in soils and sediments (Bao et al., 2018; Chen et al., 2019a, 2019b; Li et al., 2017).

The PCoA analysis showed that PFASs was not the sole influencing factor on the microbial community composition. The samples can be categorized into three groups (Figure 3A): soil samples at plots 1,2,3 (samples on site), soil samples at plots four and 7 (with greens like park or meadow), and sediment samples at plots 5 and 6. Therefore, the microbial community composition were likely to be affected by multiple factors, including vegetation cover (with green or without), types (soil or sediment), as well as PFASs.

The extreme condition-tolerant bacteria as biomarkers at fire-training zone

The LEfSe analysis confirmed the biomarkers to indicate the differences between the high PFASs group and the low PFASs group. Compared with the high PFASs group, soils with low levels of PFASs (<100 μg kg^{-1} dw) were the most enriched and showed the largest variety in indicator bacteria (Figure 5). The bacteria only including Rhodanobacteraceae, Hyphomonadaceae, D05-2, Acidobacteriia, Solibacterales, Solibacteraceae_Subgroup_3, SBR1031, Chloroflexia, and Deinococcaceae were significantly enriched ($p < 0.05$) in the high PFASs group. A strain from Rhodanobacteraceae family is acid-tolerant and alkali-tolerant (Dahal et al., 2018). Members within the Hyphomonadaceae family are optimal for living in oligotrophic habitats (Abraham and Rohde, 2013). Strains within the Deinococcaceae family, capable of DNA damage repair, are famous for their extreme radioresistance (Vujicić-Zagar et al., 2009). Members from Acidobacteria class including Solibacterales order and Solibacteraceae_Subgroup_3 family may have the capabilities to resist or transform both metal and metalloids in acidic metal-contaminated sites (Xu et al., 2021a). Various heat-tolerant strains from the Chloroflexia class have been isolated and characterized from hot springs and geothermal soils (Islam et al., 2019; Spieck et al., 2020). These bacteria that use to adapt to extreme conditions were significantly enriched in the high levels PFASs contaminated soils, suggesting that these extreme condition-tolerant (heat, acid, alkali, radio, metal, and oligotrophic tolerant) bacteria could be as biomarkers in soils at fire training zone.

Spearman correlation analysis indicated that only Chloroflexi had a significant positive correlation with PFOS ($p = 0.036$) and PFASs ($p = 0.036$) (Figure 4). This result is consistent with a previous study that the proportions of Chloroflexi had a significant correlation with PFOS (Bao et al., 2018). As discussed above, the Chloroflexia class is a biomarker at fire-training zone and has been reported to be highly resistant to high temperature stress (Islam et al., 2019; Spieck et al., 2020). The Chloroflexia belongs to Chloroflexi, thus members within the Chloroflexi may adapt to both PFASs stress and high temperature stress in this study.

Limitations of the study

In this study, we detected PFAS concentrations in the top soil and sediments at the FTA, analyzed the effect of PFASs contamination on the soil bacterial community, and identified statistically different biomarkers between groups. However, the integrated effect of PFASs and co-contaminants on soil bacteria, archaea, and fungi were not comprehensively investigated and more high-quality genomes of archaea and fungi should be assembled to further verify the effect of PFASs on the soil microbial community. Besides, more soil samples from different FTAs should be collected to further validate the effect of PFASs on soil microbial community.

STAR★METHODS

Detailed methods are provided in the online version of this paper and include the following:

- KEY RESOURCE TABLE
- RESOURCE AVAILABILITY
  - Lead contact
  - Materials availability
  - Data and code availability
- METHOD DETAILS
  - Site description and sampling
  - Samples preparation
  - PFASs standards
  - PFASs analysis
  - Soil physicochemical properties analysis
  - High-throughput sequencing
- QUANTIFICATION AND STATISTICAL ANALYSIS

SUPPLEMENTAL INFORMATION

Supplemental information can be found online at https://doi.org/10.1016/j.isci.2022.104084.

ACKNOWLEDGMENTS

This work was supported by the National Key R&D Program of China (No. 2018YFC1802500) and a special fund from the State Key Joint Laboratory of Environment Simulation and Pollution Control (20Y02ESPCT).

AUTHOR CONTRIBUTIONS

L.C. and F.Z. designed the experiments. L.C., W.X., and Z.W. were responsible for collecting samples, PFAS detection, and sequencing. L.C. conducted the experiments, performed data processing, and wrote the paper. F.Z. and G.L. helped to revise the manuscript. All authors took part in the interpretation of data.

DECLARATION OF INTERESTS

The authors declare no competing interests.

Received: September 28, 2021
Revised: February 4, 2022
Accepted: March 11, 2022
Published: April 15, 2022

REFERENCES

Aasen, E., Sørheim, R., Hartnik, N., and Kristoffer. (2008). Screening of Polyfluorinated Organic Compounds at Four Fire Training Facilities in Norway (Norwegian Environment Agency), pp. 1–88.

Abraham, W.-R., and Rohde, M. (2013). The Family Hyphomonadaceae. In The Prokaryotes: Alphaproteobacteria and Betaproteobacteria (Springer), pp. 283–299.

Ahrens, L., Benskin, J.P., Cousins, I.T., Crimi, M., and Higgins, C.P. (2019). Themed issues on per- and polyfluoroalkyl substances. Environ. Sci. Process. Impacts *21*, 1797–1802.

Anderson, R.H., Long, G.C., Porter, R.C., and Anderson, J.K. (2016). Occurrence of select perfluoroalkyl substances at U.S. Air Force aqueous film-forming foam release sites other than fire-training areas: field-validation of critical fate and transport properties. Chemosphere *150*, 678–685.

Baduel, C., Mueller, J.F., Rotander, A., Corfield, J., and Gomez-Ramos, M.-J. (2017). Discovery of novel per- and polyfluoroalkyl substances (PFASs) at a fire fighting training ground and preliminary investigation of their fate and mobility. Chemosphere *185*, 1030–1038.

Baduel, C., Paxman, C.J., and Mueller, J.F. (2015). Perfluoroalkyl substances in a firefighting training ground (FTG), distribution and potential future release. J. Hazard. Mater. *296*, 46–53.

Bao, Y., Li, B., Xie, S., and Huang, J. (2018). Vertical profiles of microbial communities in perfluoroalkyl substance-contaminated soils. Ann. Microbiol. *68*, 399–408.

Bergström, S. (2014). Transport of Per- and Polyfluoroalkyl Substances in Soil and Groundwater in Uppsala, Sweden (Swedish University of Agricultural Sciences), pp. 1–44.

Bräunig, J., Baduel, C., Barnes, C.M., and Mueller, J.F. (2019). Leaching and bioavailability of selected perfluoroalkyl acids (PFAAs) from soil contaminated by firefighting activities. Sci. Total Environ. *646*, 471–479.

Brusseau, M.L., Anderson, R.H., and Guo, B. (2020). PFAS concentrations in soils: background levels versus contaminated sites. Sci. Total Environ. *740*, 140017.

Bugna, G.C., Chanton, J.P., Stauffer, T.B., MacIntyre, W.G., and Libelo, E.L. (2005). Partitioning microbial respiration between jet fuel and native organic matter in an organic-rich long time-contaminated aquifer. Chemosphere *60*, 177–187.

Casson, R., and Chiang, S.-Y. (2018). Integrating total oxidizable precursor assay data to evaluate fate and transport of PFASs. Remediation J. *28*, 71–87.

Chea, E., and Livesay, D.R. (2007). How accurate and statistically robust are catalytic site predictions based on closeness centrality? BMC Bioinformatics *8*, 153.

Chen, L., Tsui, M., Lam, J., Hu, C., Wang, Q., Zhou, B., and Lam, P. (2019a). Variation in microbial community structure in surface seawater from Pearl River Delta: discerning the influencing factors. Sci. Total Environ. *660*, 136–144.

Chen, L., Tsui, M.M.P., Lam, J.C.W., Wang, Q., Hu, C., Wai, O.W.H., Zhou, B., and Lam, P.K.S. (2019b). Contamination by perfluoroalkyl substances and microbial community structure in Pearl River Delta sediments. Environ. Pollut. *245*, 218–225.

Dahal, R.H., Chaudhary, D.K., and Kim, J. (2018). Rhodanobacter hydrolyticus sp. nov., a novel DNA- and tyrosine-hydrolysing gammaproteobacterium isolated from forest soil. Evol. Microbiol. *68*, 2580–2586.

Dauchy, X., Boiteux, V., Colin, A., Hémard, J., Bach, C., Rosin, C., and Munoz, J.-F. (2019). Deep seepage of per- and polyfluoroalkyl substances through the soil of a firefighter training site and subsequent groundwater contamination. Chemosphere *214*, 729–737.

Filipovic, M., Woldegiorgis, A., Norström, K., Bibi, M., Lindberg, M., and Österås, A.-H. (2015). Historical usage of aqueous film forming foam: a case study of the widespread distribution of perfluoroalkyl acids from a military airport to groundwater, lakes, soils and fish. Chemosphere *129*, 39–45.

Fitzgerald, N.J.M., Temme, H.R., Simcik, M.F., and Novak, P.J. (2019). Aqueous film forming foam and associated perfluoroalkyl substances inhibit methane production and Co-contaminant degradation in an anaerobic microbial community. Environ. Sci. Process. Impacts *21*, 1915–1925.

García, R.A., Chiaia-Hernández, A.C., Lara-Martin, P.A., Loos, M., Hollender, J., Oetjen, K., Higgins, C.P., and Field, J.A. (2019). Suspect screening of hydrocarbon surfactants in AFFFs and AFFF-contaminated groundwater by high-resolution mass spectrometry. Environ. Sci. Techn. *53*, 8068–8077.

Greenblum, S., Turnbaugh, P.J., and Borenstein, E. (2012). Metagenomic systems biology of the human gut microbiome reveals topological shifts associated with obesity and inflammatory bowel disease. Proc. Natl. Acad. Sci. U S A *109*, 594–599.

Guelfo, J.L., and Higgins, C.P. (2013). Subsurface transport potential of perfluoroalkyl acids at aqueous film-forming foam (AFFF)-impacted sites. Environ. Sci. Techn. *47*, 4164–4171.

Hale, S.E., Arp, H.P.H., Slinde, G.A., Wade, E.J., Bjørseth, K., Breedveld, G.D., Straith, B.F., Moe, K.G., Jartun, M., and Høisæter, Å. (2017). Sorbent amendment as a remediation strategy to reduce PFAS mobility and leaching in a contaminated sandy soil from a Norwegian firefighting training facility. Chemosphere *171*, 9–18.

Hoisaeter, A., Pfaff, A., and Breedveld, G.D. (2019). Leaching and transport of PFAS from aqueous film-forming foam (AFFF) in the unsaturated soil at a firefighting training facility under cold climatic conditions. J. Contaminant Hydrol. *222*, 112–122.

Houtz, E.F., Higgins, C.P., Field, J.A., and Sedlak, D.L. (2013). Persistence of perfluoroalkyl acid precursors in AFFF-impacted groundwater and soil. Environ. Sci. Techn. *47*, 8187–8195.

Huang, S., and Jaffé, P.R. (2019). Defluorination of perfluorooctanoic acid (PFOA) and perfluorooctane sulfonate (PFOS) by acidimicrobium sp. Strain A6. Environ. Sci. Techn. *53*, 11410–11419.

Islam, Z.F., Cordero, P.R.F., Feng, J., Chen, Y.-J., Bay, S.K., Jirapanjawat, T., Gleadow, R.M., Carere, C.R., Stott, M.B., Chiri, E., and Greening, C. (2019). Two Chloroflexi classes independently evolved the ability to persist on atmospheric hydrogen and carbon monoxide. ISME J. *13*, 1801–1813.

Kao, C.M., and Prosser, J. (1999). Intrinsic bioremediation of trichloroethylene and chlorobenzene: field and laboratory studies. J. Hazard. Mater. *69*, 67–79.

Kärrman, A., Elgh-Dalgren, K., Lafossas, C., and Møskeland, T. (2011). Environmental levels and distribution of structural isomers of perfluoroalkyl acids after aqueous fire-fighting foam (AFFF) contamination. Environ. Chem. *8*, 372–380.

Langille, M.G.I., Zaneveld, J., Caporaso, J.G., McDonald, D., Knights, D., Reyes, J.A., Clemente, J.C., Burkepile, D.E., Vega Thurber, R.L., Knight, R., et al. (2013). Predictive functional profiling of microbial communities using 16S rRNA marker gene sequences. Nat. Biotechnol. *31*, 814–821.

Li, B., Bao, Y., Xu, Y., Xie, S., and Huang, J. (2017). Vertical distribution of microbial communities in soils contaminated by chromium and perfluoroalkyl substances. Sci. total Environ. *599–600*, 156–164.

Liu, G., Zhang, S., Yang, K., Zhu, L., and Lin, D. (2016). Toxicity of perfluorooctane sulfonate and perfluorooctanoic acid to Escherichia coli: membrane disruption, oxidative stress, and DNA damage induced cell inactivation and/or death. Environ. Pollut. *214*, 806–815.

Liu, Y., Ma, L., Yang, Q., Li, G., and Zhang, F. (2018). Occurrence and spatial distribution of perfluorinated compounds in groundwater receiving reclaimed water through river bank infiltration. Chemosphere *211*, 1203–1211.

McGuire, M.E., Schaefer, C., Richards, T., Backe, W.J., Field, J.A., Houtz, E., Sedlak, D.L., Guelfo, J.L., Wunsch, A., and Higgins, C.P. (2014). Evidence of remediation-induced alteration of subsurface poly- and perfluoroalkyl substance distribution at a former firefighter training area. Environ. Sci. Techn. *48*, 6644–6652.

Qiao, W., Xie, Z., Zhang, Y., Liu, X., Xie, S., Huang, J., and Yu, L. (2018). Perfluoroalkyl substances (PFASs) influence the structure and function of soil bacterial community: greenhouse experiment. Sci. Total Environ. *642*, 1118–1126.

Sharifan, H., Bagheri, M., Wang, D., Burken, J., Higgins, C., Liang, Y., Liu, J., Schaefer, C., and Blotevogel, J. (2021). Fate and transport of per- and polyfluoroalkyl substances (PFASs) in the vadose zone. Sci. Total Environ. *771*, 145427.

Segata, N., Izard, J., Waldron, L., Gevers, D., Miropolsky, L., Garrett, W.S., and Huttenhower, C. (2011). Metagenomic biomarker discovery and explanation. Genome Biol. *12*, R60.

Spieck, E., Spohn, M., Wendt, K., Bock, E., Shively, J., Frank, J., Indenbirken, D., Alawi, M., Lücker, S., and Hüpeden, J. (2020). Extremophilic nitrite-oxidizing Chloroflexi from Yellowstone hot springs. ISME J. *14*, 364–379.

Sun, Y., Wang, T., Peng, X., Wang, P., and Lu, Y. (2016). Bacterial community compositions in sediment polluted by perfluoroalkyl acids (PFAAs) using Illumina high-throughput sequencing. Environ. Sci. Pollut. Res. *23*, 10556–10565.

UNEP (2009). Listing of perfluorooctane sulfonic acid, its salts and perfluorooctane sulfonyl fluoride. In UNEP-POPS-COP.4-SC-4-17 (United Nations Environment Program USA), pp. 15–18.

Vujicić-Zagar, A., Dulermo, R., Gorrec, M., Vannier, F., Servant, P., Sommer, S., Groot, A., and Serre, L. (2009). Crystal structure of the IrrE protein, a central regulator of DNA damage repair in Deinococcaceae. J. Mol. Biol. *386*, 704–716.

Wang, S., Huang, J., Yang, Y., Hui, Y., Ge, Y., Larssen, T., Yu, G., Deng, S., Wang, B., and Harman, C. (2013). First report of a Chinese PFOS alternative overlooked for 30 Years: its toxicity, persistence, and presence in the environment. Environ. Sci. Techn. *47*, 10163–10170.

Wang, Z., DeWitt, J.C., Higgins, C.P., and Cousins, I.T. (2017). A never-ending story of per- and polyfluoroalkyl substances (PFASs)? Environ. Sci. Techn. *51*, 2508–2518.

Weathers, T.S., Harding-Marjanovic, K., Higgins, C.P., Alvarez-Cohen, L., and Sharp, J.O. (2016).

Perfluoroalkyl acids inhibit reductive dechlorination of trichloroethene by repressing Dehalococcoides. Environ. Sci. Techn. *50*, 240–248.

Xu, R., Sun, X., Häggblom, M.M., Dong, Y., Zhang, M., Yang, Z., Xiao, E., Xiao, T., Gao, P., Li, B., and Sun, W. (2021a). Metabolic potentials of members of the class Acidobacteriia in metal-contaminated soils revealed by metagenomic analysis. Environ. Microbiol. *24*, 803–818.

Xu, R., Tao, W., Lin, H., Huang, D., Su, P., Gao, P., Sun, X., Yang, Z., and Sun, W. (2021b). Effects of perfluorooctanoic acid (PFOA) and perfluorooctane sulfonic acid (PFOS) on soil microbial community. Microb. Ecol. 1–13. https://doi.org/10.1007/s00248-021-01808-6.

Zhang, D.-Q., Zhang, W., and Liang, Y. (2019a). Bacterial community in a freshwater pond responding to the presence of perfluorooctanoic acid (PFOA). Environ. Techn. *41*, 1–23.

Zhang, D., Zhang, W., and Liang, Y. (2019b). Distribution of eight perfluoroalkyl acids in plant-soil-water systems and their effect on the soil microbial community. Sci. Total Environ. *697*, 134146.

Zhang, L., Liu, J., Hu, J., Liu, C., Guo, W., Wang, Q., and Wang, H. (2012). The inventory of sources, environmental releases and risk assessment for perfluorooctane sulfonate in China. Environ. Pollut. *165*, 193–198.

STAR★METHODS

KEY RESOURCE TABLE

REAGENT or RESOURCE	SOURCE	IDENTIFIER
Chemicals, peptides, and recombinant proteins		
PFASs standards	Tianjin Alta scientific	N/A
VOCs standards	Tianjin Alta scientific	N/A
Solid-phase extraction column	Waters Oasis WAX cartridges	Cat#186002493
HPLC column	Thermo Fisher Scientific	Cat#068982
Methanol (HPLC grade, ≥99.9%)	Macklin	Cat#M813907
Ammonium acetate (HPLC grade, ≥99.9%)	Macklin	Cat#A801000
NH_4OH (HPLC grade,25%)	Sigma-Aldrich (Shanghai)	Cat#543830
Critical commercial assays		
Fast DNA™ spin kit	MPbio	Cat# 06,560-200
Deposited data		
Genome sequencing data	This paper	PRJNA748948
Software and algorithms		
R language version 3.3.1	R language Software Foundation	N/A
CANOCO 4.5 toolkit	CANOCO Software Foundation	N/A
NetworkX	Python Software Foundation	https://networkx.org/
Qiime version 1.9.1	Qiime Software Foundation	http://qiime.org/install/index.html
Mothur Version 1.30.2	Mother Software Foundation	https://www.mothur.org/wiki/Download_mothur
PICRUSt2 version 2.2.0	PICRUSt Software Foundation	http://picrust.github.io/picrust/
Uparse Version 7.0.1090	Uparse Software Foundation	http://www.drive5.com/uparse/
Other		
GC-FID (7890A)	Agilent	https://www.agilent.com.cn/
TOC analyzer	SHIMADZU	https://www.shimadzu.com/an/products/total-organic-carbon-analysis/toc-analysis/toc-l-series/index.html
LC-MS (Ultimate 3000/ISQ EC)	Thermo Fisher Scientific	https://www.thermofisher.cn/order/catalog/product/IQLAAAGABHFAPBMBFD
CHNS elemental analyzer	Thermo Fisher Scientific	https://www.thermofisher.cn/order/catalog/product/11206125

RESOURCE AVAILABILITY

Lead contact

Further information and requests for materials should be directed to and will be fulfilled by the lead contact, Fang Zhang (fangzhang@tsinghua.edu.cn).

Materials availability

This study did not generate new unique reagents.

Data and code availability

The accession numbers for the genome sequencing data reported in this paper NCBI: PRJNA748948. BioSample accessions: SAMN20348734 for plot 1, SAMN20348735 plot 2, SAMN20348736 for plot 3, SAMN20348737 for plot 4, SAMN20348738 for plot 5, SAMN20348739 plot 6, and SAMN20348740 for plot 7.

METHOD DETAILS

Site description and sampling

Soil and sediment samples were collected from a location at fire-training base in Shanghai, China. This base was established in December 2012 and has been used for firefighting training activities from 2013. The training areas were covered by thick concrete. Waste oil, solvents, and fuels were ignited, and subsequently extinguished using various firefighting agents, including 3 and 6% AFFFs. These AFFFs are composed of hydrocarbon surfactants, fluorocarbon surfactants, additives, stabilizers, antifreeze and so on. The detailed information of fluorocarbon surfactants was not provided from manufacturer. Wastewater from firefighting training activities was discharged into the nearby river through ditches.

Soil and sediment samples were collected in October 2019. A map of the sampling plots is presented in supplemental information (Figure S2). Soil (≈2 kg) were collected 20 cm below ground surface at concrete-free ditches (Plots 1–4) and sediments (≈1 kg) were collected at the middle of river (Plots five and 6). A control sample was collected at center of park (Plot 7). Each plot collected approximate 2 kg soil from three plots of equilateral triangle. Soil and sediment samples were stored at 4°C until use and analyzed for physicochemical properties in triplicate. Plots one to four were located the fire-fighting zones.

Samples preparation

All samples were dried by a freeze dryer prior to extraction and extracted in triplicate. The soil extraction method was similar to the approach used by Liu et al. (2018). Briefly, a 2000 mg subsample of a homogenized soil sample was placed in a 50 mL polypropylene (PP) centrifuge tube containing 15 mL of methanol. Tubes were vortexed for 30 s, sonicated for 20 min at 30–35°C. The extract was separated from the soil by centrifugation at 8000 rpm for 10 min. The supernatant was transferred to a 500 mL PP beaker with a 10 mL pipette. The extraction process was repeated two more times to ensure complete removal of all PFASs. The combined extract was diluted to 300 mL with deionized water and then was purified by a solid-phase extraction column. Waters Oasis WAX cartridges (150 mg, 6 mL) were sequentially pre-conditioned with 6 mL of 0.5% NH_4OH in methanol, 6 mL of methanol and 6 mL of deionized water. The extract was loaded into the cartridges with a flow 3–5 mL min^{-1}. The cartridges were sequentially washed with 5 mL of deionized water and 5 mL of 25 mM ammonium acetate buffer solution at pH four and vacuumed at 65 kPa to remove any residual water. The analytes were eluted 4 mL of 0.5% NH_4OH in methanol. The eluent was evaporated to dryness under a gentle stream of high-purity N_2 and resolved into 1000 μL 50:50 methanol: water for PFASs analysis.

PFASs standards

Purity corrected stock solutions of 11-analyte mixture included seven perfluoroalkyl acids (PFAAs), four perfluorinated sulfonates (PFSAs) were purchased from Tianjin Alta scientific Co., Ltd. The mixture contained perfluorobutanoic acid (PFBA), perfluoropentanoic acid (PFPeA), perfluorohexanoic acid (PFHxA), perfluoroheptanoic acid (PFHpA), PFOA, perfluorononanoic acid (PFNA), perfluorodecanoic acid (PFDA), perfluorobutanesulfonate (PFBS), perfluorohexanesulfonate (PFHxS), perfluoroheptanesulfonate (PFHpS) and PFOS.

PFASs analysis

All samples were analyzed in 1000 μL of 50:50 methanol: water. Analysis was conducted on a liquid chromatography−mass spectrometry (LC−MS, Ultimate 3000/ISQ EC, Thermo Fisher Scientific) equipped with an Acclaim RSLC 120 C18 column (2.2 μm, 2.1 mm × 100 mm). Milli-Q water containing 10 mM ammonium acetate was used as the aqueous phase (A) and the organic phase (B) was acetonitrile. The flow velocity of the mobile phase was 0.3 mL min^{-1}. The injection volume was set at 25 μL and the column temperature at 30°C. The eluent gradient started with 35% (B) for 0.5 min, followed by a linear increase in phase B from 35 to 60% (0.5–10 min). The 60% phase B was held for 2 min (10–12 min) and eventually returned to the initial conditions within 1 min and held for 2 min for equilibration during the injection interval. Detection was done by a heated electrospray ionization in the negative ion mode (V = −4.5 kV). The nebulizing gas temperature was set at 450°C. A list of MS parameters of the target analytes is included in Table S2.

Whole method LODs ranged from 0.05 to 0.95 ng g^{-1} dw (Table S3). Spike recoveries and method precision for solid sample analysis were within the range from 75% ± 4%–141% + 1% (Table S3).

Soil physicochemical properties analysis

Soil moisture content (MC) and soil organic matter (OM) were measured by loss on ignition under 105 °C for 5 h and then 550°C for 5 h. The soil pH was measured with a fresh soil/water ratio of 1:5 (v/v) by using an METTLER TOLEDO pH meter (SevenExcellence; Shanghai, China). Soil total carbon (C), hydrogen (H), sulfur (S) and nitrogen (N) were measured with a FlashSmart CHNS elemental analyzer (Thermo Fisher Scientific, Germany). Soil organic carbon (TOC) and inorganic carbon (IC) were determined using a TOC–L analyzer (SHIMADZU, Japan). The other contaminants, such as TCE, benzene, toluene, ethylbenzene, and xylenes are easy to microbial degradation were measured by GC–FID (GC 7890A, Agilent, USA). The detailed information for determining volatile organic compounds (VOCs) can be seen in the China environmental standard for Soil and Sediment-Determination of VOCs-Headspace gas chromatography (HJ-741-2015). When the amount of soil and sediment samples is 2 g, the detection limit of 37 VOCs is 0.005–0.03 mg kg^{-1}.

High-throughput sequencing

Total DNA was extracted from 10 g aliquots of samples, as described in the manual of the Fast DNA™ spin kit for soil (MPbio, USA). The concentration and purity of the extracted DNA samples were checked using a NanoDrop 2000 Spectrophotometer (Thermo Fisher Scientific, USA). The V3–V4 region of the 16S rRNA gene of bacteria was amplified using primer-set 338F–806R. High-throughput sequencing was performed using the Illumina MiSeq platform (USA). The QIIME software was used to filter and analyze the obtained original sequences (Qiime version 1.9.1). The Bray-Curtis distance constructed by the QIIME software was used to evaluate the beta diversity of the system development. The alpha diversity index of the sample data was analyzed using the Mothur software (Mothur Version 1.30.2) and the processed data was mapped using Origin (OriginPro, 2016, 64-bit). Operational taxonomic units (OTUs) were clustered with a 97% similarity cut-off using the Uparse software (Uparse Version 7.0.1090). We also used the PICRUSt2 (PICRUSt2 version 2.2.0) pipeline to predict the functional genes for metabolism of the pathway at level 3 based on 16S rRNA gene data and using the latest Kyoto Encyclopedia of Genes and Genomes (KEGG) database (Langille et al., 2013).

QUANTIFICATION AND STATISTICAL ANALYSIS

Student's t–test was used for calculating the significant difference of alpha diversity indexes between high PFAS group and low PFASs group. Kruskal-wallis was used for calculating the significant difference of bacterial functions and topological parameters between high PFASs group and low PFASs group. Principal co-ordinates analysis (PCoA) was performed by R language (version 3.3.1). The CANOCO 4.5 toolkit was conducted for and canonical correspondence analysis (CCA). The CCA analysis was carried out based on soil physicochemical properties and PFASs concentration to identify the environmental variables with significant effects on the microbial community. Relationships between bacterial composition (phylum level) and environmental variables were analyzed by Spearman correlation heatmap. Linear discriminant analysis (LDA) coupled with effect size measurements (LEfSe) analysis was performed for searching statistically different biomarkers between low PFASs group and high PFASs group (Segata et al., 2011). The co-occurrence network analysis was performed for quantifying the topological impacts of PFASs accumulations on soil bacteria by Networkx toolkit.